J. Physiol. (1983), **341**, *pp.* 59–74
With 9 text-figures
Printed in Great Britain

THE STRENGTH–DURATION RELATIONSHIP FOR EXCITATION OF MYELINATED NERVE: COMPUTED DEPENDENCE ON MEMBRANE PARAMETERS

BY H. BOSTOCK

From the Sobell Department of Neurophysiology, Institute of Neurology, Queen Square, London WC1N 3BG

(*Received 13 January 1983*)

SUMMARY

1. Thresholds to applied current pulses have been determined for the myelinated nerve model of Goldman & Albus (1968).

2. Strength–duration curves have been plotted, and compared with three strength–duration equations that have been proposed in the past. The simple, linear relation between stimulus charge and stimulus duration proposed by Weiss (1901) provided the best fit to the computed data.

3. The effects on the strength–duration relationship of changes in twelve parameters of the model were determined and expressed in terms of the strength–duration time constant and rheobasic current. The rheobase depended primarily on conductances, whereas the strength–duration time constant depended on the electrotonic time constant and also on the rate of sodium activation.

4. The model predicts strength–duration curves of the same form, for extracellular or intracellular stimulation where the external resistance is low and uniform. Tripolar stimulation, with anodes over adjacent rather than remote nodes, is predicted to result in much shorter strength–duration time constants, but with a similar sensitivity to nodal membrane parameters.

5. The limitations of strength–duration measurements on myelinated nerves are discussed in the light of these simulations.

INTRODUCTION

The relationship between the strength and the duration of a threshold stimulus to a nerve or muscle fibre preoccupied many electrophysiologists before the development of intracellular and voltage-clamp techniques (e.g. see review by Katz, 1939). One of the early investigators was Georges Weiss (1901), who obtained accurately timed, short duration stimuli, not by the usual Helmholtz pendulum, but by cutting two wires in quick succession with a bullet fired from a liquid CO_2 carbine. He found that his strength–duration data obtained from frog nerves were fitted very well by the formula:

$$Q = a + bt \tag{1}$$

(where Q is stimulus charge, t duration, and a and b constants). This simple formula was ignored by most subsequent authors, probably because no theory was available

to account for it, in contrast to the 'classical' strength–duration formula of Lapicque (1907), and the modification with two time constants due to Hill (1936), both of which were based on simple models of the excitation process. Tasaki (1939), however, reported that isolated toad fibres obeyed Weiss' formula well over a wide stimulus range, but he did not make any attempt to account for this relationship, or interpret the constants.

Following Hodgkin & Huxley's (1952) comprehensive model of the squid axon membrane, the strength–duration behaviour of uniformly excitable cables has been simulated by Cole, Antosiewicz & Rabinowitz (1955), Cooley, Dodge & Cohen (1965) and Noble & Stein (1966). The latter authors related the form of the strength–duration curves, calculated both for point polarized and uniformly polarized cables, to the current–voltage curves and to the equations of Lapicque (1907) and Hill (1936).

Frankenhaeuser & Huxley (1964) made the first calculations of membrane action potentials in myelinated nerve, based on voltage-clamp data from nodes of *Xenopus laevis* and Frankenhaeuser (1965) used this model to calculate a limited range of strength–duration data for space-clamped nodes. Propagation of impulses along model fibres with these nodal properties was simulated by Goldman & Albus (1967), using data from Tasaki (1955) for the internodes and the computing methods of Fitzhugh (1962). This model of myelinated nerve has subsequently been modified to imitate demyelination (Smith & Koles, 1970; Koles & Rasminsky, 1972; Schauf & Davis, 1974), but no simulation studies have been made of the strength–duration relationships of myelinated nerve.

The present simulation study was undertaken to fill this gap and to help understand the strength–duration curves being obtained from normal and demyelinated fibres *in vivo* (Bostock, Sears & Sherratt, 1983). The main questions to be answered by the model were: (1) how was the shape of the strength–duration curve related to the active and passive membrane properties of the fibre, particularly those that might change in demyelination? and (2) could the shape of the curve and its changes with membrane parameters, be described usefully in terms of a simple strength–duration equation?

METHODS

Nerve simulation

Since no full description was available for a model mammalian myelinated nerve, the model of Goldman & Albus (1968), based on the Frankenhaeuser & Huxley (1964) equations for *Xenopus* fibres at 20 °C was used. Following Koles & Rasminsky (1972) the standard fibre had an axon diameter of 10·5 μm, a fibre diameter of 15 μm and an internodal length of 1·38 mm. The equations were solved by 4th order Runge–Kutta integration on PDP 11/34 and CDC 7600 computers, with ten segments per internode and a fixed time increment, usually 0·2 μsec.

For the threshold determinations the simulation was limited to eleven nodes (-5 to $+5$) with the outer two clamped to the resting potential (E_r, -70 mV) and continued until (*a*) the potential at node 0 (the stimulated node) reached 60 mV above E_r, when the fibre was considered excited, or (b) the potential fell to within 10 mV of E_r after the end of the stimulus, when the fibre was considered not excited, or (c) until 250 μsec after the end of the stimulus. In the latter case the fibre was considered excited if the final potential was 30 mV or more above E_r, and not excited if it was less than 15 mV above E_r. After a run, the stimulus was raised or lowered by decreasing amounts until the threshold was determined within 0·1 %, or until the potential at node 0 was in the range 15–30 mV above E_r, 250 μsec beyond the end of the stimulus. When the program was

run on the PDP 11/34, membrane potentials were displayed and could be plotted (e.g. Fig. 2), to check the validity of the threshold estimates. Strength–duration curves were usually determined with stimuli comprising rectangular current pulses of durations 20, 40, 60, 80, 100, 150, 200, 300 and 500 μsec. When membrane parameters were altered, usually by a factor of 2, the changes were made throughout the fibre, not just to the stimulated node or its surroundings.

To provide a comparison with previous comutations, the model was extended to thirty-one nodes (-15 to $+15$) and conduction velocity estimated from the time required for the 50 mV level of the leading edge of the action potential to propagate from node 5 to node 6.

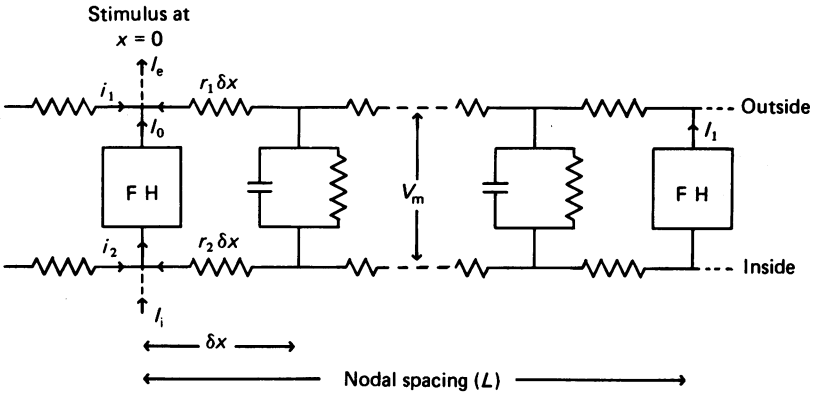

Fig. 1. Equivalent circuit of model fibre, modified from Fitzhugh (1962). The model is symmetrical about node 0 at $x = 0$. FH indicates Frankenhaeuser–Huxley (1964) membrane model at nodes of Ranvier. I_n is the membrane current at the nth node. I_e and I_i represent alternative paths for stimulating current.

Stimulation

Fig. 1. shows the equivalent circuit of part of the model axon, with two alternative methods of stimulation: withdrawal of a current I_e from the outside of node 0, as described by Fitzhugh (1962), or injection of a current I_i intracellularly. With the usual cable symbols (e.g. Hodgkin & Rushton, 1946),

$$\frac{\delta V_m}{\delta x} = \frac{\delta V_1}{\delta x} - \frac{\delta V_2}{\delta x} = r_2 i_2 - r_1 i_1 = i_2(r_1+r_2) - r_1(i_1+i_2).$$

For an externally applied current stimulus I_e (see Fig. 1):

$$I_e = 2(i_1+i_2)$$
$$I_0 = 2i_2,$$

therefore

$$I_0 = I_e \frac{r_1}{(r_1+r_2)} + \frac{2}{(r_1+r_2)} \frac{\delta V_m}{\delta x}. \tag{2}$$

For an intracellularly applied current I_i (see Fig. 1):

$$I_i = -2\,(i_1+i_2)$$
$$I_0 = I_i + 2i_2,$$

therefore

$$I_0 = I_i + \frac{2}{(r_1+r_2)} \frac{\delta V_m}{\delta x} - I_i \frac{r_1}{(r_1+r_2)}$$

which, for $r_1 \ll r_2$, reduces to

$$I_0 = I_i + \frac{2}{(r_1+r_2)} \frac{\delta V_m}{\delta x}. \tag{3}$$

Comparing eqns. (2) and (3), withdrawal of a current I_e from the outside of node 0 is equivalent to injection of current $I_e r_1/(r_1+r_2)$ intracellularly and Fitzhugh (1962) termed this quantity the 'effective stimulating current' (I_{eff}). To avoid having to assume an arbitrary value for the external

longitudinal resistance r_1, stimulating currents are always stated in terms of I_{eff} and otherwise r_1 was assumed small compared with r_2.

In this standard method of stimulation, a net charge of $I_e.T$ for a stimulus of duration T was withdrawn from the centre of the fibre, the circuit being completed via the ends of the fibre, which were at fixed potential. This differed in two ways from the experimental situation used by Bostock *et al.* (1983), which avoided any accumulation of stimulus charge. They used a balanced tripolar stimulus, to improve the spatial resolution of their threshold measurements and this was stimulated by subtracting half the stimulating current from node 1 (and by symmetry from node -1), i.e.

$$I_1 = \frac{\{V_m(L+\delta x) + V_m(L-\delta x) - 2V_m(L)\}}{(r_1+r_2)\,\delta x} - \frac{I_{eff}}{2}.$$

Secondly, Bostock *et al.* (1983) used an a.c. coupled stimulating circuit, to allow membrane current recording through the same electrodes and this was stimulated by letting

$$I_{eff} = I_s.e^{-t/RC} \quad \text{for} \quad 0 < t < T$$

and

$$I_{eff} = I_s\,(e^{-t/RC} - e^{(T-t)/RC}) \quad \text{for} \quad t > T,$$

where T is the nominal stimulus duration, I_s the nominal effective stimulating current and RC the stimulator time constant.

RESULTS

Verification of the computations

For the standard conditions, integration of the equations on the PDP 11/34 and the CDC 7600 computers both gave internodal conduction times of 73·4 μsec, in good agreement with the figure of 74 μsec given by Koles & Rasminsky (1972).

A further check on the passive cable properties of the model was made by running a simplified version for which an exact solution was available. If myelin conductance can be ignored and the nodal resistance (R_n) is constant, the input conductance of the fibre (G_{in}) should be given by:

$$G_{in} = \sqrt{(1+4R_n/r_2L)}/R_n.$$

With the active permeabilities set to zero, R_n is 40·02 MΩ and r_2L is 17·53 MΩ, (where L is the nodal spacing) so that G_{in} should be 79·5 nS. For the thirty-one-node model, simulation without myelin conductance gave G_{in} as 79·7 nS and reduction to eleven nodes (-5 to $+5$) only changed this to 79·9 nS. Incorporation of the standard value for myelin conductance increased these figures by 8%.

Threshold behaviour of the model

Fig. 2. shows calculated potentials at the stimulated node for a 100 μsec stimulus. Threshold was approached by repeatedly splitting the difference between the best estimate above threshold and the best estimate below threshold, until the required accuracy was reached. Similar behaviour of a uniformly excitable model nerve was shown by Cooley *et al.* (1965).

Form of the strength–duration relationship

Strength–duration data for the standard nerve are plotted in Fig. 3*A* with current and in Fig. 3*B* with charge as the ordinate. To test the shape of the curve, two points (for 40 and 500 μsec stimuli) were used to generate three curves. The continuous line, straight in Fig. 3*B*, was generated from Weiss' formula (eqn. 1). For comparison

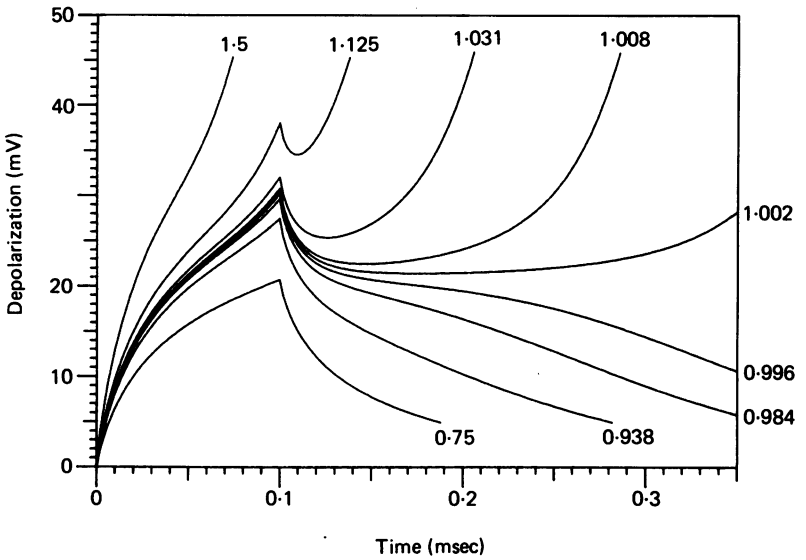

Fig. 2. Potential wave forms at node 0 for stimuli of 100 μsec duration and standard parameter set, showing successive approximations to threshold. Figures indicate stimulating currents as fractions of threshold.

between equations, Weiss' constants a and b can be replaced by the rheobasic current (I_{rh}) and the strength–duration time constant (τ_{sd}), defined by Noble & Stein (1966) as the ratio between the charge threshold for very short stimuli and the rheobase. Weiss' equation then becomes:

$$Q = I_{rh}\,(t+\tau_{sd}). \tag{4}$$

In so far as Weiss' equation applies, therefore, the rheobase is given by the slope of the line in Fig. 3*B* and the strength–duration time constant by the intercept on the charge axis.

The long-dashed lines in Fig. 3*A* and 3*B* were generated from Lapicque's (1907) 'classical' strength–duration equation, which may be written as:

$$I = \frac{I_{rh}}{1-e^{-t/\tau_{sd}}}. \tag{5}$$

Hill's (1936) equation for constant current pulses was:

$$I = \frac{I_{rh}(1-\kappa/\lambda)}{e^{-t/\lambda}-e^{-t/\kappa}}, \tag{6}$$

where κ represented the membrane time constant and λ the time constant of accomodation. All the curves generated by this equation fall between the limits given by the long-dashed lines, when $\lambda/\kappa \to \infty$ and Hill's equation reduces to Lapicque's and the short-dashed lines, when $\lambda/\kappa \to 1$ and Hill's equation reduces to:

$$I = I_{rh}.\tau_{sd}/t.e^{-t/e.\tau_{sd}} \quad \text{for} \quad 0 < t < e.\tau_{sd} \tag{7}$$

or

$$I = I_{rh} \quad \text{for} \quad t > e.\tau_{sd}.$$

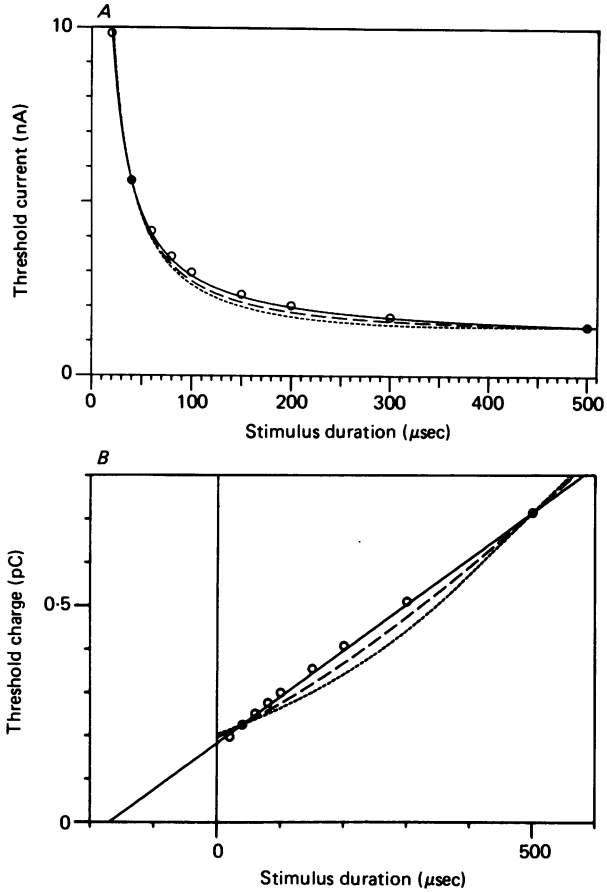

Fig. 3. *A*, strength–duration data for standard model nerve, with curves generated to fit two points (filled circles) according to eqns. (4) (continuous line), (5) (long-dashed line) and (6) (short-dashed line). *B* same, plotted as charge thresholds. Intercept of straight line on zero charge axis gives estimated strength–duration time constant.

It is clear from Fig. 3 that of the three equations Weiss' provides the best fit to the model for the standard parameter set and the same has been true for all the variations of the model tested. Weiss' equation also provides the best extrapolation to longer and shorter stimuli, e.g. the threshold current to a 1 msec stimulus was 1·26 nA, while the values predicted by the three equations were 1·25 nA (Weiss), 1·40 nA (Lapicque) and 1·4–1·44 nA (Hill). There are invariably some systematic deviations from Weiss' equation, in particular it over-estimates the threshold charge for very short stimuli, but if Weiss' equation is fitted to the nine data points by linear regression of Q on t, the fitted points deviate by only 2·3 % on average (i.e. r.m.s. percentage error). The best-fitting line is not significantly different from the line fitted to two points in Fig. 3*B*, and yields estimates for I_{rh} of 1·07 nA and for τ_{sd} of 173 μsec.

Effects of various parameters on strength–duration curves

To ascertain how the strength–duration relationship was related to the membrane properties and other parameters of the model, threshold determinations for the same stimulus durations were repeated, changing one parameter at a time and then the strength–duration time constant and rheobase were estimated from the regression of Q on t as above. The results are summarized in Table 1, which also shows the effects of the same changes on conduction velocity.

TABLE 1. Effects of changes in the model nerve on the strength–duration relationship and on conduction velocity

	Change in parameter	Percentage change		
		τ_{sd}	I_{rh}	Velocity
Passive nodal parameters				
Nodal capacitance	×1/2 ×2	−16 +29	+1 −1	+17 −21
Leak conductance	×1/2 ×2	+31 −26	−28 +52	+14 −25
Passive internodal parameters				
Myelin capacitance	×1/2* ×2	−16 +26	0 +1	+20 −23
Myelin conductance	×1/2 ×2	+4 −7	−4 +8	+3 −5
Axoplasmic resistivity	×1/2* ×2	0 +4	+45 −30	+48 −35
Active nodal parameters				
Max. sodium conductance	×1/2 ×2	+8 −3	+10 −10	−24 +23
Max. potassium conductance	×0	+1 —	−1 —	0 —
Rate constants:				
Sodium activation	×1/2 ×2	+21 −17	+8 −4	−31 +33
Sodium inactivation	×1/2 ×2	+1 −1	−1 +2	+3 −6
Potassium	×1/2 ×2	0 0	0 0	0 −1
Nodal width	×1/2 ×2	+18 −9	−21 +35	+10 −19
Temperature 1 (see text)	+10 +20	−17 −38	−5 −3	+30 +52
Temperature 2 (see text)	+10 +20	−31 −60	+32 +92	+40 +76

* Denotes that the time increment for integrations had to be reduced for computational stability.

Passive nodal and internodal parameters. The effects of changes in nodal capacitance and nodal leak conductance on the strength–duration relationship are illustrated in Fig. 4. Doubling the time constant of the nodal membrane in each case increases, but only by about 30%, the strength–duration time constant (see Tables 1 and 2). On Lapicque's (1907) simple treatment of the excitation process, the nerve was assumed to charge passively until a fixed voltage threshold for the all-or-none spike discharge was reached. The strength–duration time constant in his formula, like κ in Hill's equation (6), was therefore presumed to correspond to the time constant for passive charging of the fibre. This is very far from being the case with the model, and the fallacy of the assumption of a sharp voltage threshold is illustrated in Fig. 5.

The passive depolarizations shown in the dashed lines in Fig. 5 are not exponential, because of the cable properties of the fibre, neither do they follow the time course expected for point polarization of a uniform cable (i.e. $\mathrm{erf}\sqrt{t/\tau}$, derived in Hodgkin & Rushton, 1946). They have an intermediate shape (Fig. 6), since the input

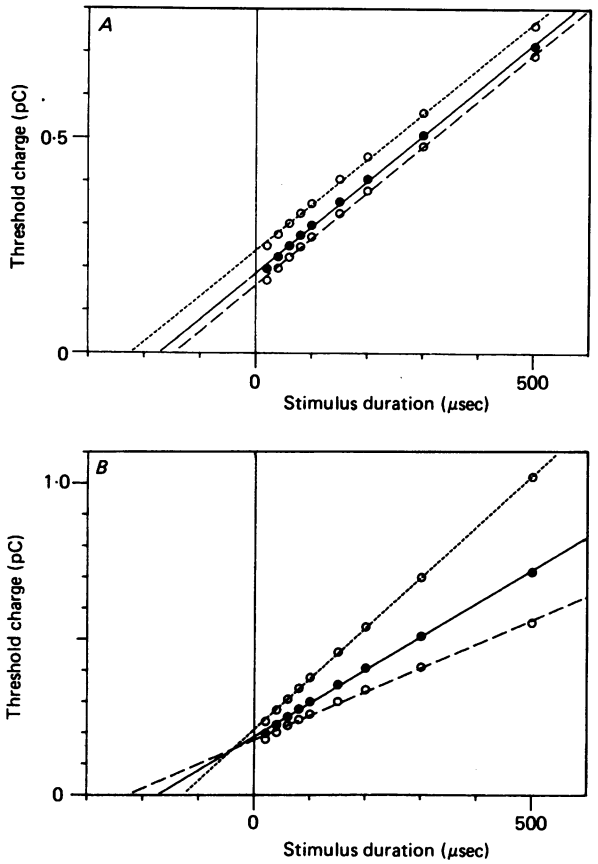

Fig. 4. *A* effect of change in nodal capacitance on charge–duration relationship. Filled circles indicate standard model, fitted with continuous line (τ_{sd} = 173 μsec, I_{rh} = 1·07 nA). Open circles fitted with long-dashed line (τ_{sd} = 147 μsec, I_{rh} = 1·08 nA), show effect of halving and those fitted with short-dashed line (τ_{sd} = 224 μsec, I_{rh} = 1·07 μsec) show effect of doubling nodal capacitance. *B*, effects of changing nodal leak conductance, plotted similarly. Long-dashed line: leak conductance ×1/2 (τ_{sd} = 228 μsec, I_{rh} = 0·77 nA). Short-dashed line: leak conductance ×2 (τ_{sd} = 128 μsec, I_{rh} = 1·63 nA).

impedance is partly that of a node, and partly that of a cable. A suitable intermediate shape is provided by Rall's (1960) equation for a motoneurone, if a dendritic to somatic conductance ratio of 10 is arbitrarily assumed. The passive depolarizations are, however, also fitted adequately by the much simpler expression:

$$V = \frac{I.t}{G_{in}(t+k)}, \tag{8}$$

where V is the depolarization and G_{in} is the input conductance. The constant k has the dimensions of time, and like the time constant for an exponential depolarization, it is the ratio between the equilibrium depolarization and the initial rate of depolarization. It can therefore be regarded as an electrotonic time constant, τ_{el}:

i.e.
$$\tau_{el} = \frac{(V)_{t\to\infty}}{\left(\frac{dV}{dt}\right)_{t\to 0}}. \tag{9}$$

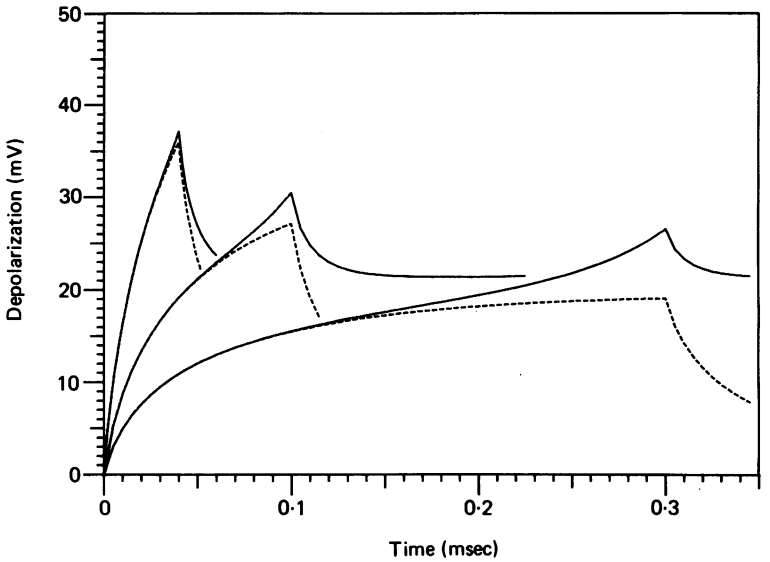

Fig. 5. Potential wave forms at stimulated node for stimuli very close to threshold of 40, 100 and 300 μsec duration, showing variation in 'threshold'. Dashed lines indicate electrotonic responses, obtained by setting potential dependent permeabilities to zero.

Eqn. (8) can therefore be rewritten to resemble eqn. (4):

$$Q = V.G_{in}\,(t+\tau_{el}). \tag{10}$$

On the assumption of a sharp, instantaneous threshold for excitation, we would therefore expect τ_{sd} to equal τ_{el}, but for the standard parameters in Fig. 6, τ_{el} is 34 μsec and τ_{sd} is 173 μsec. Although very different in absolute magnitude, these two time constants are closely related, provided sodium conductance parameters are not changed. The relationship is almost linear (see Fig. 7) and accounts for the effects of changes in nodal capacitance, nodal leakage conductance and myelin conductance on the strength–duration time constant. The straight line in Fig. 7 has the formula:

$$\tau_{sd} = 104 + 2{\cdot}07.\tau_{el}. \tag{11}$$

This formula also accounts quite well for the effects of changes in nodal width, since these are dominated by the passive membrane properties. Doubling the nodal width, but keeping the specific membrane properties the same, reduces the electrotonic time constant by 19%, which according to eqn. (11) should reduce the strength–duration time constant by 7%. Simulation indicated a reduction of 9% (Table 1).

The rheobasic current is that which produces a critical depolarization if maintained long enough, while a maintained current produces a passive depolarization proportional to the input conductance of the fibre. It was therefore not surprising to find that changes in passive nodal and internodal parameters altered the rheobase in proportion to the input conductance. Thus halving the nodal leak conductance reduced the input conductance by 27% and the rheobasic current by 28%. To put this another way, with the standard sodium channel parameters, the rheobasic current was always the minimum current required to produce an electrotonic depolarization of about 12·6 mV.

Active nodal parameters. Of the active nodal parameters, the strength–duration

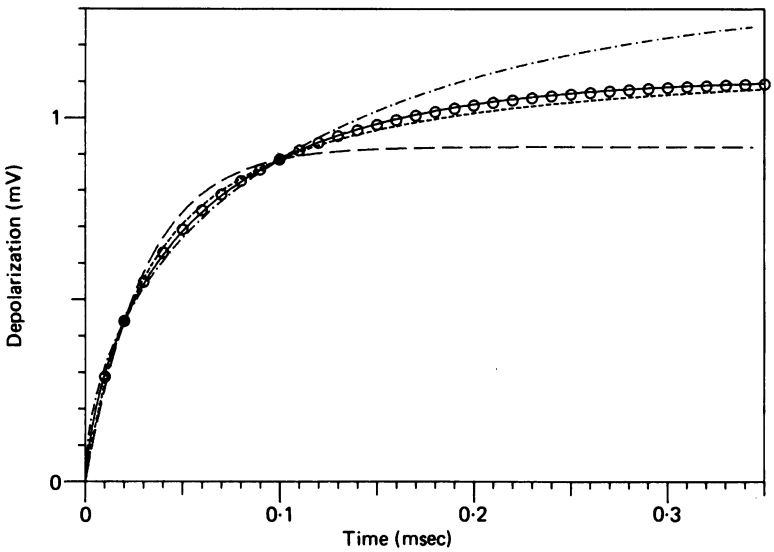

Fig. 6. Time course of electrotonic depolarization of model nerve. Circles show potentials at stimulated node for a subthreshold current step (0·1 nA). The four curves have been fitted to the same two points (filled circles; 20 and 100 μsec). Three of the curves correspond to Rall's (1960) equation for the soma of a motoneurone, for different values of the dendritic–somatic conductance ratio ρ. The long-dashed curve is an exponential, corresponding to uniform depolarization of a cable (or to $\rho = 0$); the dot-dashed line corresponds to point polarization of a uniform cable (or to $\rho = \infty$) and the continuous line corresponds to $\rho = 10$. The short-dashed line is given by eqn. (8).

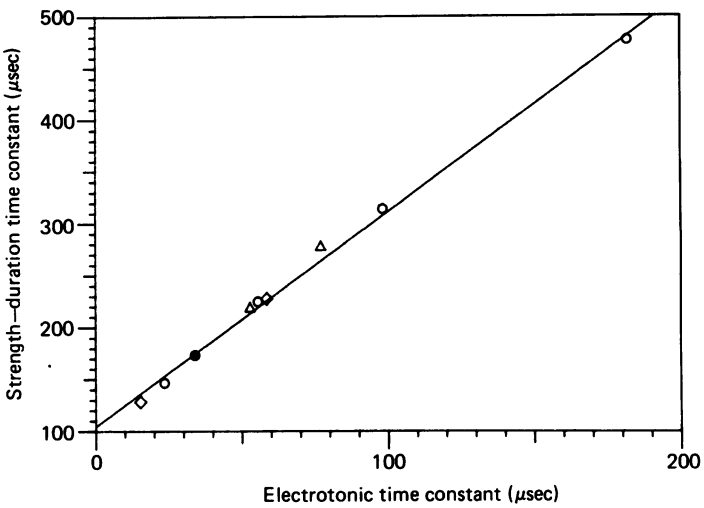

Fig. 7. Relationship between electrotonic and strength–duration time constants for different passive membrane parameters. Filled circle; standard model. Open circles: nodal capacitance $\times 1/2$, $\times 2$, $\times 4$, $\times 8$. Diamonds: leak conductance $\times 1/2$, $\times 2$. Triangles: myelin capacitance $\times 2$, $\times 4$. The straight line is the best (least-squares) fit to the five circles (eqn. 11).

relationship is most sensitive to changes in the rate of sodium activation. Speeding up sodium channel opening reduces the discrepancy between the electrotonic and strength–duration time constants. The effects of changes in sodium inactivation are negligible, as is the contribution of potassium channels (Table 1).

Temperature. There is some uncertainty in the literature as to how the effects of temperature on myelinated nerve should best be simulated. Hutchinson, Koles & Smith (1970) made careful measurements on single fibres of *Xenopus laevis* and found that between 20 and 30 °C, velocity increased on average by 33 %. They attempted to simulate this, using the Goldman & Albus (1967) model, and Q_{10}s for rate constants and maximum permeabilities taken from Frankenhaeuser & Moore (1963) and Frankenhaeuser (1965). This model nerve increased in velocity by 99 % between 20 and 30 °C and failed to conduct at 35 °C. Their computations were probably in error, since the present, similar model with the same Q_{10}s increases its velocity by a more realistic 30 % between 20 and 30 °C and conducts above 40 °C (see temperature 1, Table 1). Schauf & Davis' (1974) model behaved similarly. Also, Moore, Joyner, Brill, Wakman & Najar-Joa (1978), who used Hodgkin–Huxley rather than Frankenhaeuser– Huxley kinetics, obtained a velocity increase of about 32 % between 20 and 30 °C when rate constants only were changed.

Moore *et al.* (1978) argued that the temperature dependence of the axoplasmic conductance should be taken into account and when they incorporated a Q_{10} of 1·3 for this the 20–30 °C velocity increase went up to 68 %, considerably higher than the experimental values of 33 % (Hutchinson *et al.* 1970) or about 29 % (Frankenhaeuser & Waltman, 1959) and further addition of a Q_{10} of 1·4–1·5 for maximum ionic conductances hardly altered this. They did not explicitly mention their assumptions about leak conductance. It was found that inclusion of a Q_{10} of 1·3 for axoplasmic conductance and a Q_{10} of 1·4 for the leakage conductance (similar to the Q_{10}s of the voltage-dependent conductances) gave a figure of 40 % for the 20–30 °C velocity increase (see temperature 2, Table 1). The effects of these different assumptions on the strength–duration curve were marked (Table 1). The strength–duration observations on rat nodes (Bostock *et al.* 1983) were fitted better by the first assumptions (temperature 1), of changes in the rate constants and maximum permeabilities only.

Mode of stimulation

It has already been shown (see Methods) that intracellular application of stimulating current is equivalent to extracellular withdrawal of current, if allowance is made for the short-circuiting factor. The method of stimulating the model nerve was also altered in two ways to allow a better comparison with the experimental observations (Bostock *et al.* 1983).

Stimulator time constant. The effect of a.c. coupling on the strength–duration curve was, as expected, to increase the threshold to longer stimuli. For example, a 1 msec stimulator time constant raised the current threshold of the standard nerve to a 500 μsec stimulus by 26 % (see Fig. 8*A*). When these thresholds were plotted as charges, however, it was found that the points lay within 3 % of those for normal d.c. stimulation (Fig. 8*B*). When Weiss' formula was fitted to the data in Fig. 8*B*, the strength–duration time constant was found to be increased by only 7 %, while the rheobase was virtually unchanged (within 2 %).

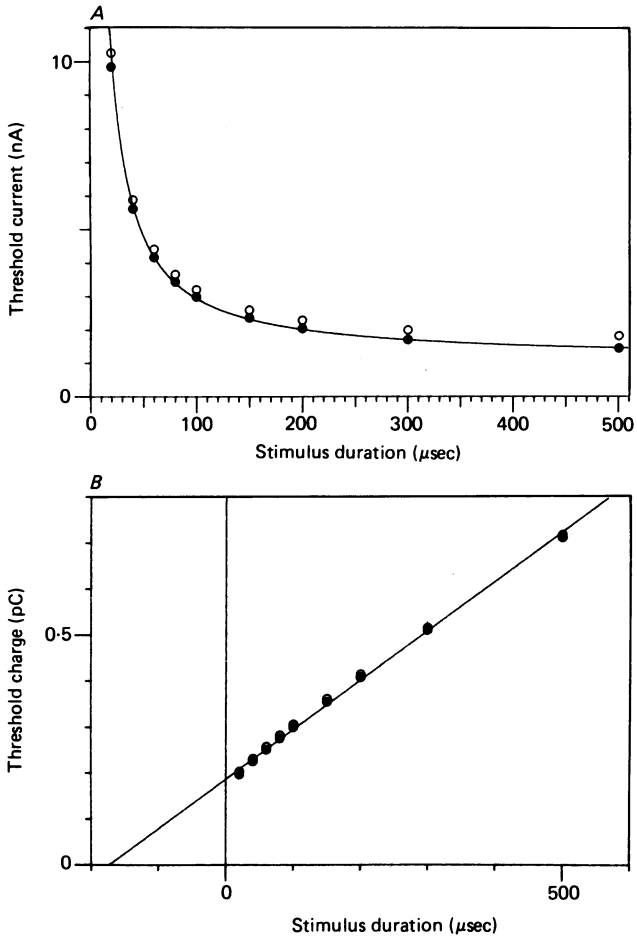

Fig. 8. *A*, strength–duration data for a.c. coupled stimulation with 1 msec time constant (open circles) compared with standard model (filled circles and curve). *B*, same, plotted as charge thresholds.

Tripolar stimulation. The effect of tripolar stimulation, with anodes over nodes ± 1, was to reduce the electrotonic time constant considerably (Fig. 9 and Table 2). This is easily understood from the definition of electrotonic time constant (eqn. 9), since the initial rate of depolarization at node 0 is unaffected by the siting of the anodes, but the final depolarization is much reduced by the anelectrotonus. The strength–duration time constant was not reduced as much as the electrotonic time constant, as expected from Fig. 7 and the effects of changing nodal membrane parameters were not very different (in percentage terms) from the normal 'monopolar' stimulation. The properties of the internodal myelin sheath were, however, less important in the case of tripolar stimulation (Table 2).

DISCUSSION

In this paper the form of the strength–duration relationship for myelinated nerve and the factors affecting it, have been explored with the aid of a computer model.

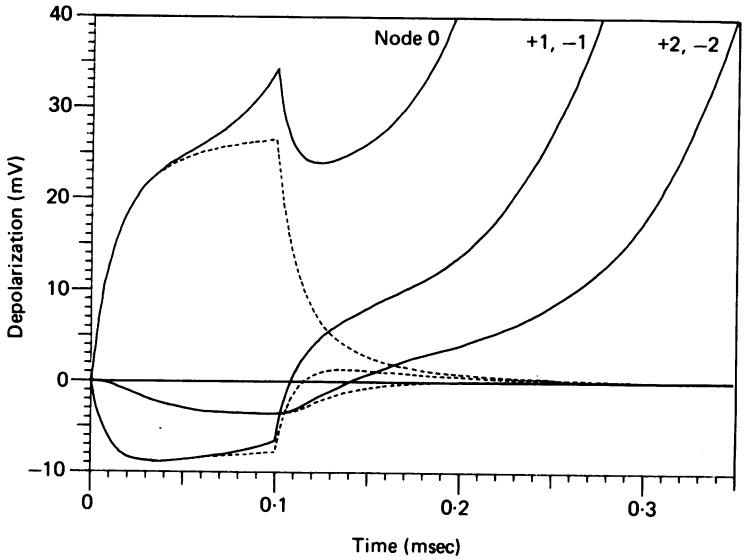

Fig. 9. Potential wave forms at nodes −2 to +2 for 100 μsec tripolar stimulus just above threshold. Cathode over node 0, and balanced anodes over nodes ±1. Dashed lines indicate electrotonic responses, obtained by setting potential-dependent permeabilities to zero.

TABLE 2. Time constants

		Percentage change on doubling	
	μsec	Nodal capacitance	Myelin capacitance
Time constant of nodal membrane	66	+100	0
Time constant of myelin sheath	464	0	+100
'Monopolar' stimulation			
Electrotonic time constant	34	+63	+55
Strength–duration constant	173	+29	+26
Tripolar stimulation			
Electrotonic time constant	8·2	+113	+57
Strength–duration constant	99	+25	+17

The only previous study of this kind was by Frankenhaeuser (1965), who also used the Frankenhaeuser & Huxley (1964) model for nodal membrane, but in that case the membrane was assumed to be space clamped and no allowance was made for the cable properties of the fibre. The properties of the internode have already been shown to be of great importance for the determination of conduction velocity (Moore *et al.* 1978) and they also affect the strength–duration relationship.

The form of the strength–duration relationship depends not only on the cable properties of the fibre, as well as on the node, but on the method of stimulation. An important early observation was that the strength–duration time constant (or chronaxie) varied with the effective size of the stimulating electrode (Davis, 1923; Grundfest, 1932) and this helped disprove Lapicque's (1926) suggestion that chronaxie was a fundamental property of a fibre. Noble & Stein (1966), in their theoretical analysis, have treated the difference in strength–duration curves between point-

polarized and uniformly polarized cables. With a myelinated fibre, however, polarization is readily applied effectively at a node, when electrode size should not be a crucial variable. Moreover, (as shown in Methods), intracellular or extracellular stimulation of a node should be related simply by the short-circuiting factor. This leaves one important source of variation, the position of the anode(s), treated here by the extreme cases of two anodes either at the ends of the fibre ('monopolar stimulation') or at nodes adjacent to the cathodal node ('tripolar stimulation').

With both methods of stimulation it was surprising to find that the strength–duration curves were fitted best, not by the conventional, exponential strength–duration equations of Lapicque (1907) or Hill (1936), but by the older and simpler eqn. (1) of Weiss (1901). For the nine selected stimulus durations, regression of stimulus charge on stimulus duration gave correlation coefficients of 0·9991 for 'monopolar' and 0·9996 for 'tripolar' stimulation. Since Weiss' equation described the strength–duration data so well, the two parameters (strength–duration time constant and rheobasic current) as defined by eqn. (4) were then used to describe the effects on the strength–duration behaviour of changing single parameters of the model. Weiss' equation was originally proposed on empirical grounds, and it has been used here simply because of its efficacy in summarizing strength–duration data with an acceptable degree of accuracy.

The parameters of the model that affected the strength–duration curves were divided into those which altered the subthreshold (electrotonic) responses and those which affected the sodium current (except for temperature, which affected both). An electrotonic time constant was defined, to allow comparison between the effects of different nodal and internodal parameters on the time course of passive depolarizations. It was found that changes in the strength–duration time constant were simply related to the electrotonic time constant, if sodium channel behaviour was kept constant. Under the same conditions, the rheobasic current was proportional to the input conductance of the fibre.

These simulations were undertaken primarily to help understand recordings being made from mammalian fibres *in vivo* and especially the large increases in strength–duration time constant accompanying paranodal demyelination (Bostock *et al.* 1983). It is unfortunate that the membrane parameters of voltage-clamped mammalian nodes have not yet been published in full, so that Goldman & Albus' (1968) nerve model was used, based on toad fibres at 20 °C. The main changes required to simulate the mammalian fibres better (Chiu, Ritchie, Rogart & Stagg, 1979) are: (1) removal of the voltage-dependent potassium and non-specific conductances (which should not affect strength–duration behaviour): (2) faster sodium inactivation (which should not affect strength–duration behaviour) and (3) a shift of the sodium permeability curve in the hyperpolarizing direction (which should have an effect similar to low calcium). At the higher temperature of the experimental preparation (30–37 °C), the strength–duration time constant should be reduced and also the discrepancy between τ_{sd} and τ_{el}. With these modifications, the results in Table 1 cannot be expected to apply accurately to mammalian nerve, but they should give a rough guide. In particular, they indicate that paranodal demyelination would reduce, rather than increase τ_{sd} if the exposed paranodal membrane were similar to nodal membrane. The large increases observed in fibres treated with diphtheria toxin (Bostock *et al.* 1983) are

only readily explained if the extra membrane contributes a large capacitance, but little extra leak conductance. A long time constant for paranodal membrane exposed by diphtheria toxin has been measured more directly in single rat fibres by Brismar (1981).

This study has shown clearly, for the first time, how strength–duration behaviour should be related to the electrotonic and voltage-dependent properties of myelinated nerve. The value of strength–duration measurements is clearly limited, since they depend on so many membrane parameters. On the other hand, strength–duration measurements, like those of conduction velocity, can readily be made on undissected nerves *in vivo*, but unlike conduction velocity measurements they relate specifically to the part of the nerve stimulated.

REFERENCES

Bostock, H., Sears, T. A. & Sherratt, R. M. (1983). The spatial distribution of excitability and membrane current in normal and demyelinated mammalian nerve fibres. *J. Physiol.* **341**, 41–58.

Brismar, T. (1981). Electrical properties of isolated demyelinated rat nerve fibres. *Acta. physiol. scand.* **113**, 161–166.

Chiu, S. Y., Ritchie, J. M., Rogart, R. B. & Stagg, D. (1979). A quantitive description of membrane currents in rabbit myelinated nerve. *J. Physiol.* **292**, 149–166.

Cole, K. S., Antosiewicz, H. A. & Rabinowitz, P. (1955). Automatic computation of nerve excitation. *J. Soc. ind. appl. Math.* **3**, 153–172.

Cooley, J., Dodge, F. & Cohen, H. (1965). Digital computer solutions for excitable membrane models. *J. cell. comp. Physiol.* **66**, Suppl. 2., 99–108.

Davis, H. (1923). The relationship of the 'chronaxie' of muscle to the size of the stimulating electrode. *J. Physiol.* **57**, 81–82*P*.

Fitzhugh, R. (1962). Computation of impulse initiation and saltatory conduction in a myelinated nerve fiber. *Biophys. J.* **2**, 11–21.

Frankenhaeuser, B. (1965). Computed action potential in nerve from *Xenopus laevis*. *J. Physiol.* **180**, 780–787.

Frankenhaeuser, B. & Huxley, A. F. (1964). The action potential in the myelinated nerve fibre of *Xenopus laevis* as computed on the basis of voltage clamp data. *J. Physiol.* **171**, 302–315.

Frankenhaeuser, B. & Moore, L. E. (1963). The effect of temperature on the sodium and potassium permeability changes in myelinated nerve fibres of *Xenopus laevis*. *J. Physiol.* **169**, 431–437.

Frankenhaeuser, B. & Waltman, B. (1959). Membrane resistance and conduction velocity of large myelinated nerve fibres from *Xenopus laevis*. *J. Physiol.* **148**, 677–682.

Goldman, L. & Albus, J. S. (1968). Computation of impulse conduction in myelinated fibres: theoretical basis of the velocity-diameter relation. *Biophys. J.* **8**, 596–607.

Grundfest, H. (1932). Excitability of the single fibre nerve–muscle complex. *J. Physiol.* **76**, 95–115.

Hill, A. V. (1936). Excitation and accommodation in nerve. *Proc. R. Soc.* B **119**, 305–355.

Hodgkin, A. L. & Huxley, A. F. (1952). A quantitative description of membrane current and its application to conduction and excitation in nerve. *J. Physiol.* **117**, 500–544.

Hodgkin, A. L. & Rushton, W. A. H. (1946). The electrical constants of a crustacean nerve fibre. *Proc. R. Soc.* B **133**, 444–479.

Hutchinson, N. A., Koles, Z. J. & Smith, R. S. (1970). Conduction velocity in the myelinated nerve fibres of *Xenopus laevis*. *J. Physiol.* **208**, 279–289.

Katz, B. (1939). *Electric excitation of nerve*. London: Oxford University Press.

Koles, Z. J. & Rasminsky, M. (1972). A computer simulation of conduction in demyelinated nerve fibres. *J. Physiol.* **227**, 351–364.

Lapicque, L. (1907). Recherches quantitatives sur l'excitation électrique des nerfs traitée comme une polarisation. *J. Physiol., Paris* **9**, 622–635.

Moore, J. W., Joyner, R. W., Brill, M. H., Waxman, S. D. & Najar-Joa, M. (1978). Simulations of conduction in uniform myelinated fibres: relative sensitivity to changes in nodal and internodal parameters. *Biophys. J.* **21**, 147–160.

NOBLE, D. & STEIN, R. B. (1966). The threshold conditions for initiation of action potentials by excitable cells. *J. Physiol.* **187**, 129–162.

RALL, W. (1960). Membrane potential transients and membrane time constants of motoneurons. *Expl Neurol.* **2**, 503–532.

SCHAUF, C. L. & DAVIS, F. A. (1974). Impulse conduction in multiple sclerosis: a theoretical basis for modification by temperature and pharmacological agents. *J. Neurol. Neurosurg. Psychiat.* **37**, 152–161.

SMITH, R. S. & KOLES, Z. J. (1970). Myelinated nerve fibres: computed effect of myelin thickness on conduction velocity. *Am. J. Physiol.* **219**, 1256–1258.

TASAKI, I. (1939). The strength–duration relation of the normal, polarized and narcotized nerve fiber. *Am. J. Physiol.* **125**, 367–379.

TASAKI, I. (1955). New measurements of the capacity and the resistance of the myelin sheath and the nodal membrane of the isolated frog nerve fibre. *Am. J. Physiol.* **181**, 639–650.

WEISS, G. (1901). Sur la possibilité de rendre comparables entre eux les appareils servant à l'excitation electrique. *Archs ital. Biol.* **35**, 413–446.